Геология и геофизика, 2018, т. 59, № 6, с. 756—772
УДК 551.14(514)

СЕДИМЕНТОЛОГИЯ И СИКВЕНС-СТРАТИГРАФИЯ РЕТРОГРАДАЦИОННОЙ СИСТЕМЫ КОНУСОВ ВЫНОСА В НИЖНЕТРИАСОВЫХ ОТЛОЖЕНИЯХ РАЙОНА МАБЭЙ В ДЖУНГАРСКОМ БАССЕЙНЕ (*Северо-Западный Китай*)

Б. Пэн[1,2,3], Ч. Цзинь[1,2], Ц. Ван[1,2], Х. Цзя[1,2], С. Чжу[1,2], Т. Чан[1,2], К. Юань[1,2]

[1]*State Key Laboratory of Petroleum Resource and Prospecting, Beijing, 102249, China*
[2]*College of Geosciences, China University of Petroleum, Beijing, 102249, China*
[3]*Shanxi Provincial Land Engineering Construction Group Co. Ltd, Xi'an, 710075, China*

Седиментология и сиквенс-стратиграфия ретроградационной системы конусов выноса в нижнетриасовых отложениях района Мабей Джунгарского бассейна на северо-западе Китая были исследованы с использованием сейсмических данных, диаграмм каротажа и данных анализа кернов, дополненных данными о современном осадконакоплении и результатами экспериментов в гидрометрических лотках. В нижнем триасе в районе Мабей преобладают конусы выноса, состоящие из дельтовой равнины (включающей субаэральный поток обломочного материала, разветвленное русло, береговые отложения конгломерата и пойму), авандельты (включающей конгломератную отмель и песчаную отмель) и продельты. Разветвленные русла формируются в период низкого паводка. Береговые отложения конгломерата образуются в период паводка и занимают большую часть долины конуса выноса. Конгломератные и песчаные отмели формируются поверхностными потоками, втекающими в озера, и имеют пластообразную форму. Разветвленные русла, конгломератные и песчаные отмели образуют высокопористые пласты. Исследования выявили один продолжительный цикл базового уровня (LSC1), три цикла базового уровня средней продолжительности (MSC1, MSC2 и MSC3) и пятнадцать кратковременных циклов базового уровня. Цикл MSC1 включает преимущественно равнину конуса выноса, в цикле MSC2 доминирует авандельта, и в цикле MSC3 преобладают авандельта и продельта. Ближнесреднедальний стратиграфический тренд показывает общую ретроградационную каротажную модель. Строение стратиграфических толщ контролируется корреляцией между изменением уровня воды в озере и поступлением осадочного материала. Быстрое повышение уровня воды в озере, опережающее скорость поступления осадочного материала, приводит к ретроградационной системе конусов выноса.

Ретроградационные конусы выноса, сиквенс-стратиграфия, нижний триас, район Мабей, бассейн Джунгар

SEDIMENTOLOGY AND SEQUENCE STRATIGRAPHY OF A RETROGRADATIONAL FAN-DELTA SYSTEM WITHIN THE LOWER TRIASSIC IN THE MABEI AREA, JUNGGAR BASIN (*northwestern China*)

B. Peng, Z. Jin, J. Wang, H. Jia, X. Zhu, T. Chang, and K. Yuan

The sedimentology and sequence stratigraphy of a retrogradational fan-delta system within Lower Triassic in the Mabei area of Junggar Basin in northwestern China were investigated using seismic, well log, and core data, complemented by the modern deposition and a flume tank experiment. The Lower Triassic in the Mabei area is dominated by fan deltas, which are composed of fan-delta plain (including subaerial debris flow, braided channel, conglomerate overbank, and floodplain), fan-delta front (including conglomerate shoal and sandy shoal), and prodelta. The braided channels form during the low flood period. The conglomerate overbanks form during the flood period and occupy most part of the fan-delta plain. The conglomerate shoals and sandy shoals form by a sheet flow prograding into lakes and occur as a sheet. The braided channels, conglomerate shoals, and sandy shoals are easy to form high-porosity reservoirs. One long-term base level cycles (LSC1), three middle-term base level cycles (MSC1, MSC2, and MSC3), and fifteen short-term base level cycles are identified. MSC1 is dominated by the fan-delta plain; MSC2 is dominated by the fan-delta front; and MSC3 is dominated by the fan-delta front and prodelta. The stratigraphy shows a proximal-middle-distal trend demonstrating an overall retrogradation stacking pattern. The sequence architecture is controlled by an interplay between lake level changes and sediment supply. The quick rise in the lake level and the creation of accommodation outpacing the rate of sediment supply result in a retrogradational fan-delta system.

Retrogradational fan deltas, sequence stratigraphy, Lower Triassic, Mabei area, Junggar Basin

1. INTRODUCTION

Sequence stratigraphy originates from seismic stratigraphy; and has become a new branch of geology through combining conventional stratigraphy, sedimentology, and some other disciplines. Sequence stratigraphy could not only provide an effective method in basin analysis, but also could interpret sedimentary systems,

✉e-mail: 43493022@163.com
DOI: 10.15372/GiG20180602

lithofacies, and their relationships (Catuneanu 2006; Evans 1993; Galloway 1989; Mitchum 1985; Posamentier et al. 2009; Zecchin and Catuneanu 2015). Sequence stratigraphy has been playing an increasingly important role in the exploration of petroleum and natural gas (Galloway 1989; Pöppelreiter and Aigner 2003; Zecchin and Catuneanu 2015). Fan-delta systems are widely spread in the margin of basins, and are important reservoirs for hydrocarbon accumulation (Dortz et al. 2011; Pöppelreiter and Aigner 2003). However, the studies concerning depositional model of fan-delta have remaining controversies (Gómez-Paccard et al. 2012; Horton B K 1996; McConnico and Bassett 2007; Park et al. 2013), and the dilemma of high-resolution sequence stratigraphy within coarse-grained deposits, especially within alluvial-fan system and fan-delta system, cannot be well resolved (Burns et al. 1997; Galloway 1976; L pez-Blanco et al. 2000; Zhang et al. 2015a).

The Mabei area, a target of hydrocarbon exploration dominated by coarse-grained successions, is located in the northwestern margin of Junggar basin, northwestern China; and has already entered middle stage of developing period(Song et al. 2009; Xian et al. 2008; Yuanjiang et al. 2007).However, due to its complicated tectonic and sedimentary characteristics, few detailed researches concerning sequence stratigraphy have been launched in this area, and the depositional model also has controversies (Carroll et al. 1990; Carroll and Graham 1995; He et al. 2013; Lichun and Jun 2007; Xian et al. 2008; Zhenyu et al. 2005). Therefore, this study aimed to analyze the sequence stratigraphic and sedimentary characteristics of Lower Triassic in Mabei area based on a lot of well-logging data, 3D seismic data and core data under the principles of high-resolution sequence stratigraphy and sedimentology. Furthermore, a modern deposition and a flume tank are added for the explanation of sedimentary characteristics.

2. GEOLOGICAL SETTING

The Mabei area is located in the northwestern Mahu Sag of Junggar Basin in northwestern China (Fig. 1). The Mabei area is about 1000km^2, and adjoins the Kexia fault belt which is manifested by large number of east-west-trending low-middle-angle thrust faults (Fig. 1C). The Lower Triassic Baikouquan formation (T1b) is the focus of this study (Fig. 2). The T1b in the Mabei area is a gentle monocline. The T1b directly overlapped the unconformity between Permian and Triassic.

The lacustrine basin infill of the northwestern margin of the Mahu Sag is subdivided into four main units: (i) a lowermost group composed of clastic rocks with some volcanoclastic rocks in the lower part; (ii) a group that includes sandstone, conglomerate, siltstone, mudstone, and shale; and (iii & iv) groups consisting of sandstone, conglomerate, siltstone, and mudstone (Carroll and Graham 1995; Feng et al. 2015). The T1b belongs to the lowermost part of the second group. From Permian to Cretaceous, the age of continental successions was studied: the lowermost group is Permian (~to 250.0Ma), the second group is Triassic (~250.0—208.0Ma), the third group is Jurassic (~208.0—145.6Ma), and the uppermost group is Cretaceous (He et al. 2013). The stratigraphic architecture of Baikouquan Formation has been extensively documented by Xian et al. (2008).

3. DATABASE AND METHODS

The study utilizes a comprehensive approach that integrates seismic interpretation and wireline log analysis, with characterization and petrographic studies of cores. The basic data include nearly 1000 km^2 three dimensional seismic data, wireline log data from 94 wells, about 220 m cores, grain-size data from 95 samples, and porosity from 85 samples. The data of seismic, wireline log, grain size and porosity come from the Xinjiang Oilfield, CNPC. Stratigraphy and depositional cross-sections along and across the depositional dip were constructed to delineate the vertical and lateral distribution of fan-delta facies. A fan-delta distribution model was established. Depositional sequences stratigraphy in the study area were identified, mainly based on seismic reflection and termination patterns these were further constrained by wireline log and core data along key seismic profiles.

Except of the subsurface data from the study area, a modern deposition and a flume tank experiment were design to understand the distribution and formation of fan-delta clastic bodies in the study area. During the formation of the fan delta in the study area, the palaeogeomorphology is a gentle slope (Jia et al. 2016; Zhang et al. 2015). Therefore, a gentle-slope fan delta was simulated in a flume where a three-dimensional coordinate system was established to facilitate data acquisition and recording. Furthermore, because the paleoclimate of T1b is arid (Wang 1994; Jia, 2016), a modern arid gentle-slope alluvial fan, located in south of Junggar Basin, was chosen to analysis the fan-delta plain sedimentary characteristics. The fan-delta plain has the same sedimentary characteristics as the alluvial fan (Whipple and Dunne 1992; Carroll et al. 1990; Nemec and Steel 1984; Gloppen and Steel 1981; Larsen and Steel 1978).

4. DEPOSITIONAL SYSTEMS

Three primary facies, fan-delta plain (including subaerial debris flow, braided channel, conglomerate overbank and floodplain), fan-delta front (including conglomerate shoal and sandy shoal) and prodelta are iden-

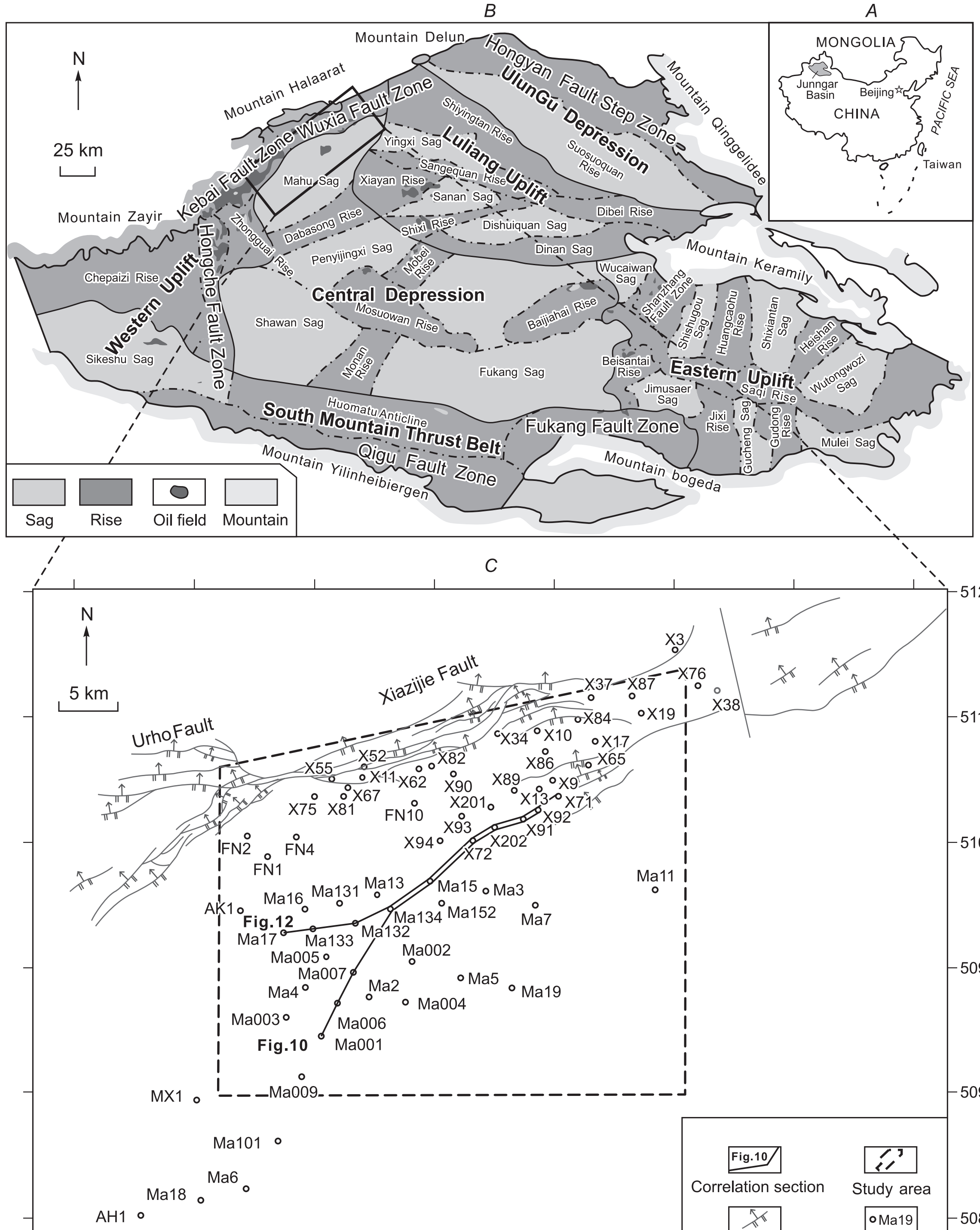

Fig. 1. Location and geological setting of the study area, Junggar basin. Modified from Jia et al. A shows the location of the Junggar Basin in China; B shows the internal units in the Junggar Basin; C shows the details of the study area.

tified on the basis of their color, lithologies, texture, sedimentary structure, wireline log patterns, facies successions and physical property (Fig. 3). Oil has been found in braided channel, conglomerate shoal and sandy shoal deposits. The distributional pattern of these facies associations is illustrated (Fig. 4, 12).

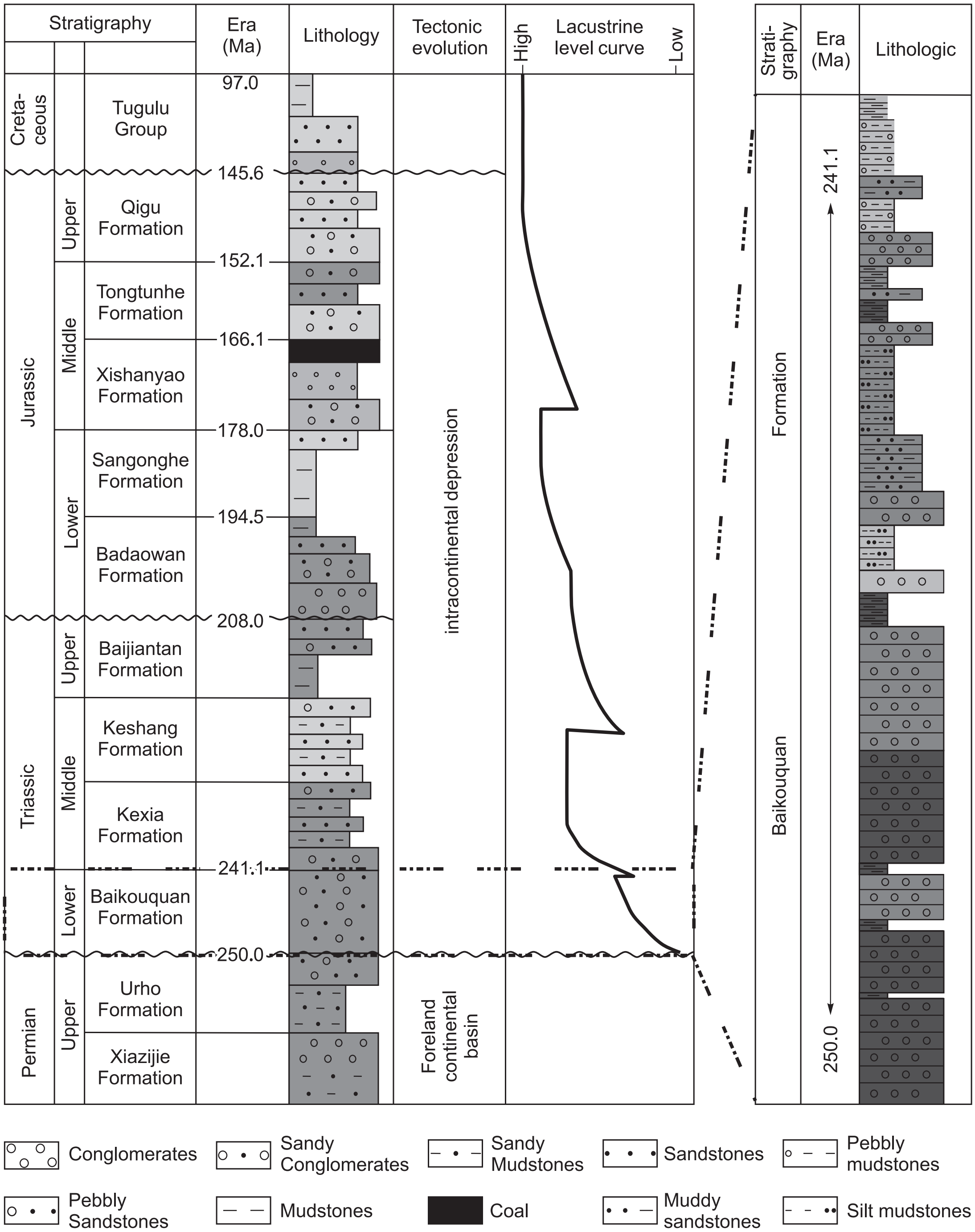

Fig. 2. Chronostratigraphy of Northwestern Junggar Basin. Modified from Jia et al. (2016). The chronostratigraphy is based on He et al. (2013). The lacustrine level curve are based on Zhao et al. (1992)

4.1 Subaerial Debris Flow Facies

4.1.1 Description

The subaerial debris flow is characterized by poor-sorted and matrix-supported conglomerate. The color of the matrix in the conglomerates is brown, and the conglomerates in this facies is poor-rounded and massive bedding (Fig. 5, E). There are no fossils found in this facies. The subaerial debris flow shows middle-amplitude box-shaped RT (Fig. 3). The grain-size accumulation probability curve has only one sub-populations (Fig. 6, B). The porosity is usually 4 to 8%.

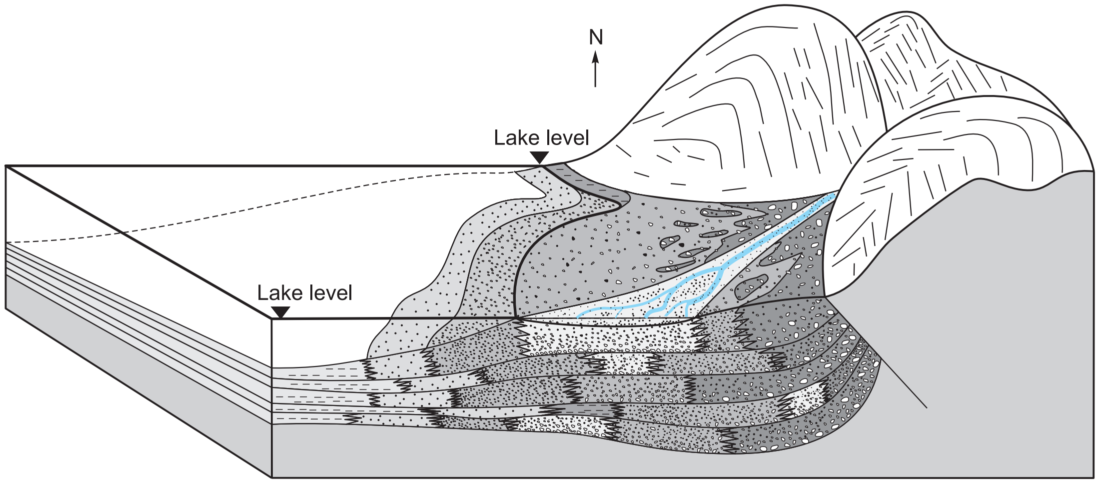

Subfacies	Prodelta	Fan delta front		Fan delta plain			
Microfacies	prodelta	sandy shoal	conglomerate shoal	floodplain	conglomerate overbank	braided channel	subaerial debris flow
Color	dark gray	gray-green	gray-green	brown	brown	brown	brown
Transport medium	traction current	traction current	traction current	traction current	traction current	traction current	gravity current
Grain size	mud	sand	gravel	mud	gravel	gravel	from gravel to mud
Structure	horizontal bedding	parallel bedding, cross bedding	massive bedding, cross bedding	massive bedding, mud-crack	massive bedding, cross bedding, imbricate arrangement	cross bedding, parallel bedding, scoured structure	massive bedding, random arrangement
Txeture	well-sorted	well-sorted clast-supported	well-sorted poor-rounded clast-supported	well-sorted	middle-sorted poor-rounded clast-supported	well-sorted, poor-rounded, clast-supported	poor-sorted, poor-rounded, matrix-supported
Well logs	short-amplitude tooth-like	middle-amplitude funnel or bell-shaped	broad-amplitude box or bell-shaped	short-amplitude tooth-like	broad-amplitude box or bell-shaped	broad-amplitude box or bell-shaped	middle-amplitude box-shaped
Electrifacies							
Examples	Ma134	Ma133	Ma16	Xia8	Ma15	Ma3	Xia74
Porosity							

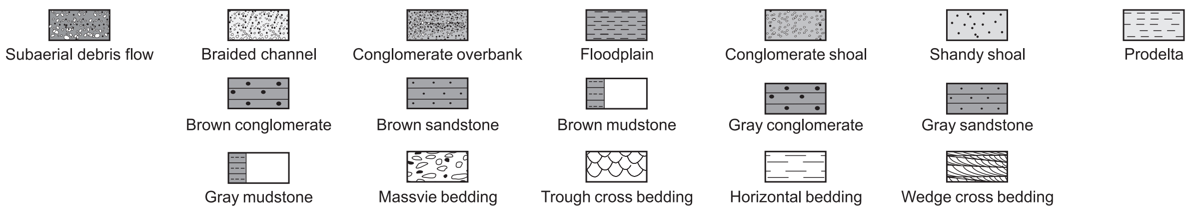

Fig. 3. Lower Triassic fan-delta comprehensive depositional characteristics in Mabei area, Junggar basin.

4.1.2 Interpretation

The poor-sorted and matrix-supported sediments and one sub-population in the grain-size accumulation probability curve indicate the gravity flow deposition. No fossils and brown matrix in this facies suggest that the formation of this facies is in the subaerial and oxidized environment.

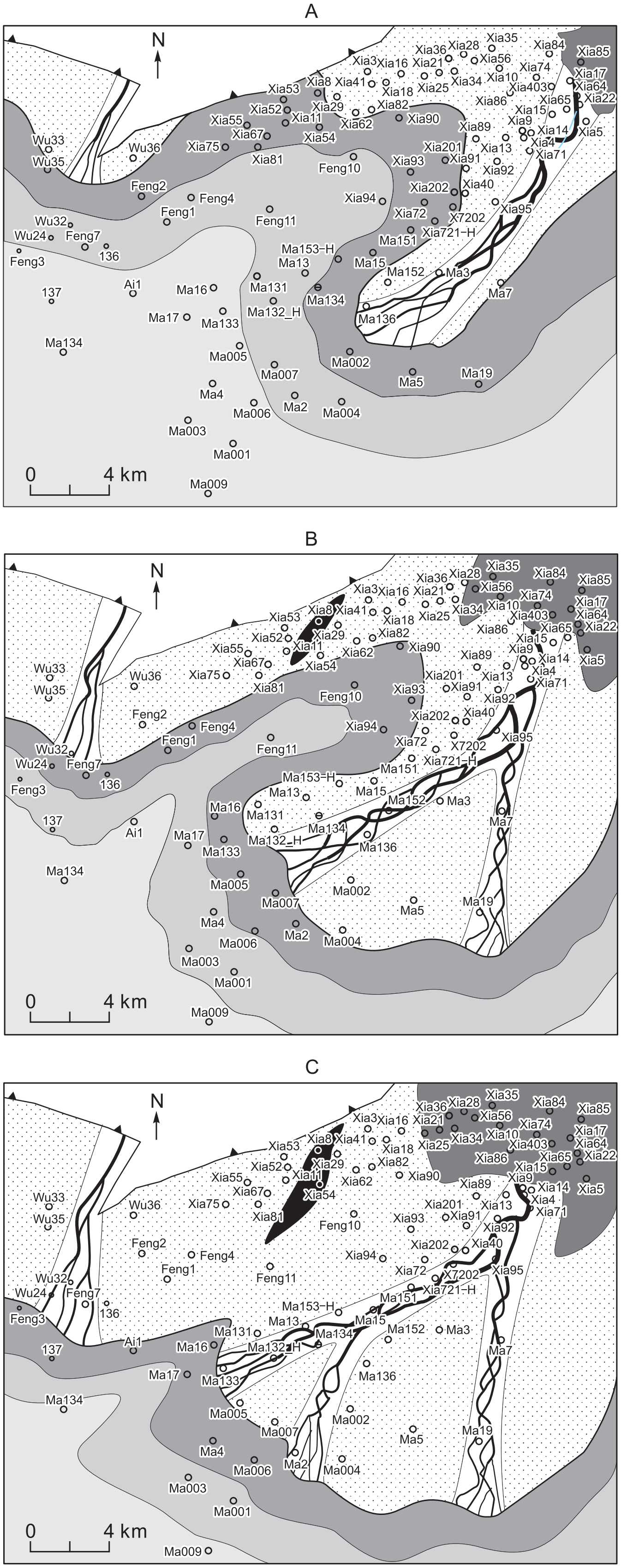

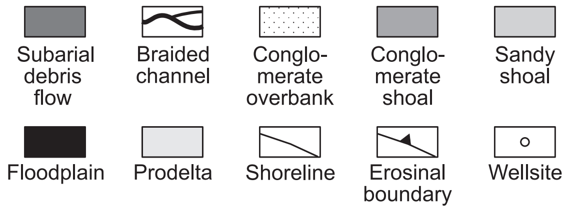

Fig. 4. Sedimentary facies map of T1b in the Mabei area. (A) Middle-term base level cycles 3; (B) Middle-term base level cycles 2; (C) Middle-term base level cycles 1.

The predominant facies were delta plain (including subaerial debris flow, braided channel and floodplain) and delta front (including conglomerate shoal and sandy shoal). The delta plain was deposited on the northeast. The delta front was deposited on the southwest. The conglomerate shoal and sandy shoal were deposited generally as a sheet, and the braided channel as a narrow belt. The conglomerate overbank was deposited around the braided channel as a sheet.

4.1.3 Formation

The subaerial debris flow facies forms during the flood period. When gravel, sand, and clay in the flood are massive enough, high viscosity and high-density debris flow are generated. The debris flow is distributed on the root of fan.

4.2 Braided Channel Facies

4.2.1 Description

The braided channel facies is characterized by well-sorted, poor-rounded and clast-supported conglomerates and pebbly sandstones. The sedimentary structures of the braided channel include trough cross bedding, tabular cross bedding (Fig. 5, A), parallel bedding (Fig 5, B), and scoured structure (Fig 5, C). There are no fossils found in this facies. The braided channel demonstrates broad-amplitude box-shaped or bell-shaped RT (Fig. 3). The grain-size accumulation probability curve possesses two sub-populations, one saltation sub-population and one suspended sub-population (Fig. 6, A). The porosity of braided channels is usually 8 to 12% (Fig. 3).

4.2.2 Interpretation

The poor-rounded coarse-grained sediments indicate a relatively short transportation distance. The well-sorted coarse-grained sediments indicate a relatively steady and continuous hydrodynamics. The common appearance of parallel bedding, cross bedding and scoured structure in conglomerates is considered as depositing in relative strong hydrodynamics (Celmmensen, 1978; Fraaser and Hester, 1977; Jiang, 2003; Tucker, 2003). One saltation sub-population and one suspended sub-population in the grain-size accumulation probability curve represent the channelized deposition (Visher, 1969). Accordingly, this facies is considered as a braided channel deposited in fan-delta plains.

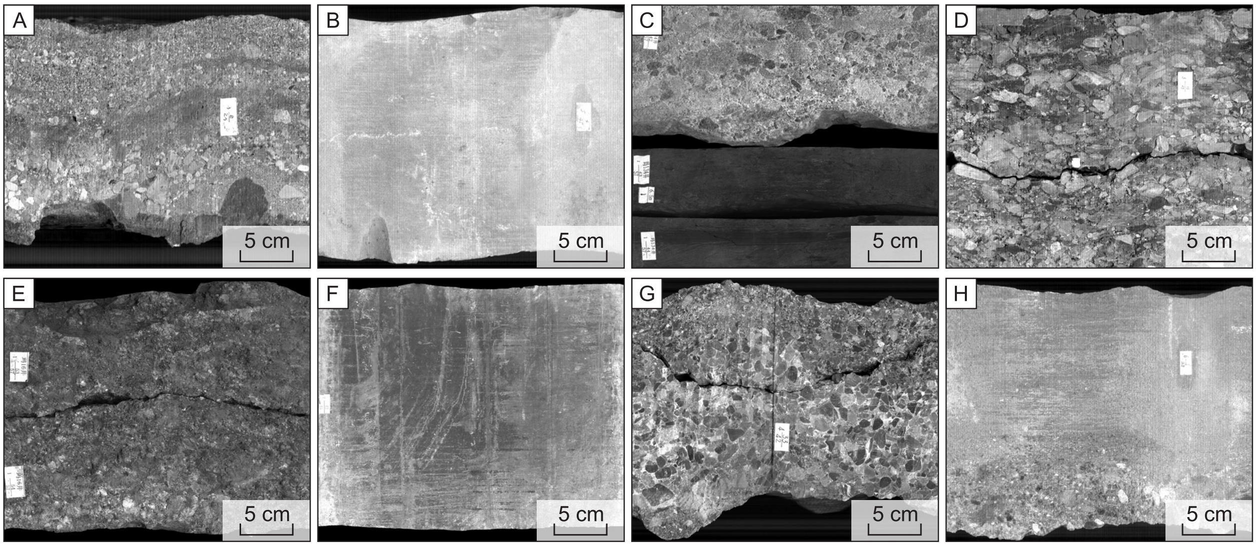
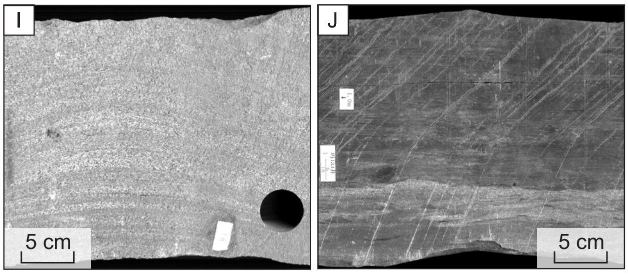

Fig. 5. 360° scanning core photographs showing different sedimentary structures in different facies in the T1b in the Mabei area.

(A) Cross bedding in greyish-brown conglomerates. From Well Ma005 at 3349.5m. (B) Paralell bedding in grey well-sorted sandstones. From Well Ma13 at 3107.0m. (C) Scour surface in brown conglomerates. From Well Ma134 at 3177.3m. (D) Massive bedding in brown conglomerates. From Well Ma134 at 3177.0m. (E) Massive bedding in brown poor-sorted conglomerates. From Well Ma16 at 3222.5m. (F) Massive bedding in brown mudstones. From Well Ma15 at 3263.0m. (G) Massive bedding in greyish-green well-sorted conglomerates. From Well Ma132 at 3261.0m. (H) Grade bedding in grey well-sorted sandstones. From Well Ma4 at 3605.0m. (I) Cross bedding in grey well-sorted sandstones. From Well Ma002 at 3092.0m. (J) Horizontal bedding in black mudstones from Well Ma133 at 3137.5m.

4.2.3 Formation

The braided channel forms during the low flood period. According to the flume tank experiment, after the flood period, due to the decline of volume and velocity and the formation of continuously braided fluid flow, the sediments of the flood period are reworked, generating the braided channels (Fig. 7, B). The construction or deposition of the fan delta occurs primarily during the flood period and the erosion or reworking of sediments occurs primarily during the low flood period. The flood period is dominated by the sheet flow; the low flood period is dominated by the channelize flow (Fig. 7, A, B). Laterally, the braided channels are distributed on the center line of a fan nearby as a belt (Fig. 7, B).

According to the modern deposition, the formation of braided channel is same with the flume tank experiment. The braided channel forms during the low flood period. After the flood period, the sediments of the flood period are reworked, generating the braided channels (Fig. 8). The braided channel is better sorted than the conglomerate overbank (Fig. 8).

4.3 Conglomerate Overbank Facies

4.3.1 Description

The conglomerate overbank is characterized by middle-sorted and clast-supported conglomerates. The sedimentary structures of the conglomerate overbank include massive bedding (Fig 5, D), imbricate arrangement and cross bedding. The conglomerates are poor-rounded. There are no fossils in this facies. The color of the matrix in this conglomerates mainly is brown. In the RT log curves, the conglomerate presents broad-amplitude box-shape or bell-shape patterns. The porosity of conglomerates in this facies is usually 6 to 10%.

4.3.2 Interpretation

The poor-rounded coarse-grained sediments indicate a relatively short transportation distance, and, the poor-sorted coarse-grained sediments indicate a relatively non-steady hydrodynamics. The common appearance

Fig. 6. Grain-size accumulation probability curve showing different hydrodynamics.

Φ = –n; D = 2^n; D is particle diameter. (A) curve represents channelized deposition. (B) curve represents gravity flow deposition.(C) curve represents relatively weak tractive flow.

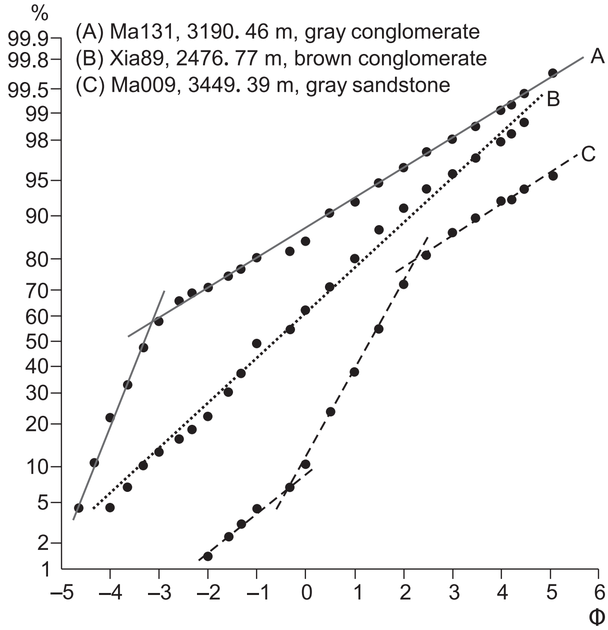

of massive bedding, cross bedding and imbricated in conglomerates is considered as depositing in relative strong hydrodynamics (Celmmensen, 1978; Fraaser and Hester, 1977; Jiang, 2003; Tucker, 2003). No fossils and brown matrix in the conglomerates suggest that formation of the conglomerate overbank is in the subaerial and oxidized environment.

4.3.3 Formation

According to the flume tank experiment and the modern deposition, the conglomerate overbank forms during the flood period, in which the flood carries an abundance of clastic sediments like a sheet (Fig. 7, A). Laterally, the conglomerate overbank is distributed like a sheet, and occupies the major portion of the fan-delta plain (Fig. 7, A, Fig. 8, A). Vertically, the conglomerate overbank and the braided channel appear alternately (Fig.8C). These suggest that episodic overbank deposition is a dominant mechanism of delta-plain aggradation. During the flood period, the sheet flow predominates on the fan-delta plain forming the conglomerate overbank; during the low flood period, the channelized flow predominates on the fan-delta plain forming the braided channel.

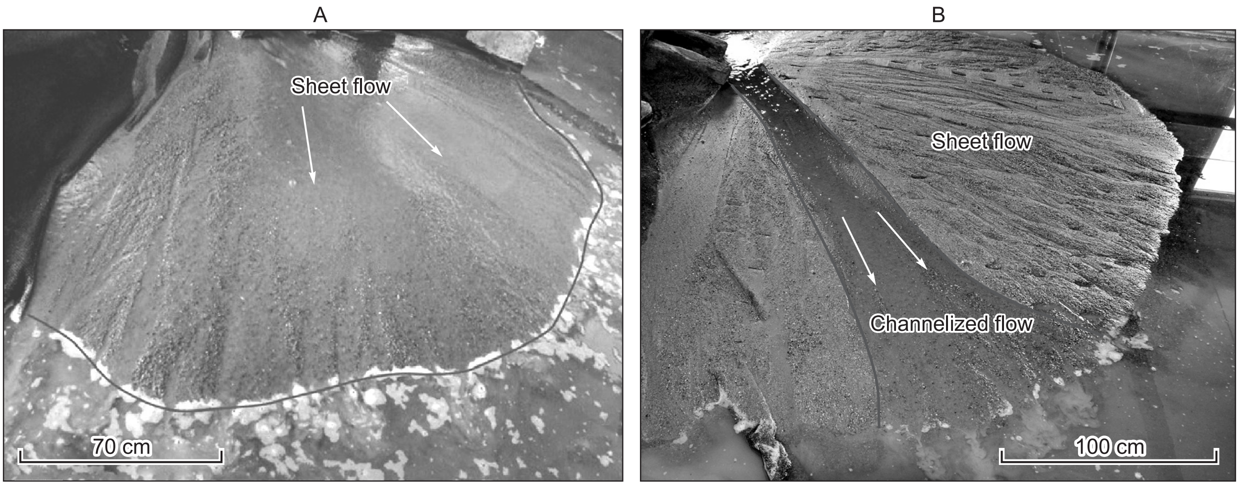

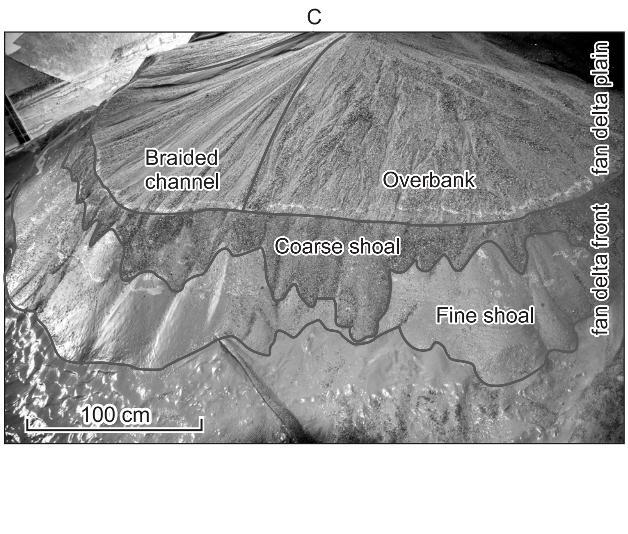

Fig. 7. Different geomorphic characteristics during different periods in the flume tank.

(A) The flood period. The fan-delta plain is dominated by sheet flow like a sheet. (B) The low flood period. The braided channel forms during this period. (C) After water discharge. The fan-delta plain can be divided into two parts, braided channel and overbank. The fan-delta front can be divided into two parts, coarse shoal and fine shoal.

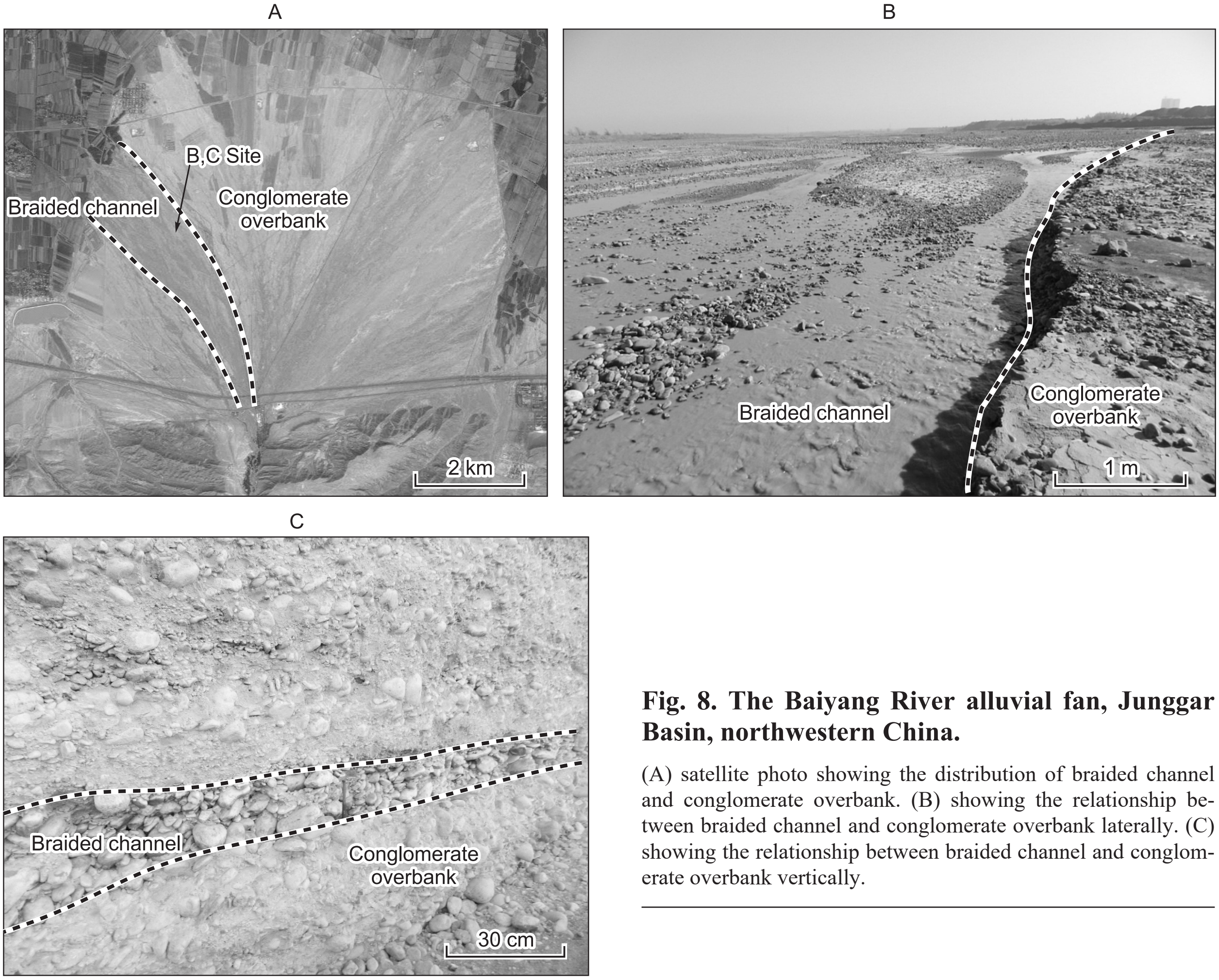

Fig. 8. The Baiyang River alluvial fan, Junggar Basin, northwestern China.

(A) satellite photo showing the distribution of braided channel and conglomerate overbank. (B) showing the relationship between braided channel and conglomerate overbank laterally. (C) showing the relationship between braided channel and conglomerate overbank vertically.

4.4 Floodplain Facies

4.4.1 Description

The floodplain is characterized by brown mudstones, intercalated with the conglomerate overbank. The mudstone is generally 2 to 5 m thick. The sedimentary structures of floodplain include massive bedding (Fig. 5, F) and mud crack structure. In the RT logs, the floodplain facies generally displays a short-amplitude tooth-like pattern (Fig. 3).

4.4.2 Interpretation

The dominance of mudstones in this facies indicates a low-energy environment. The brown mudstones indicate the subaerial and oxidized environment.

4.4.3 Formation

The mudstones are deposited on the circumjacent of each fan, outer fan (Fig. 9). The farther sediment is transported in fluid, the weaker the energy of the fluid is. When the energy of the fluid drops to a certain level, the suspending clay in the fluid is depos-

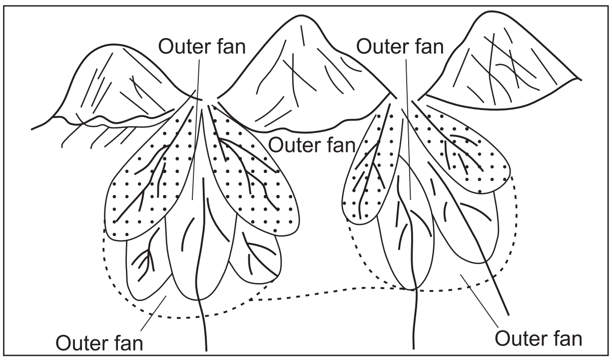

Fig. 9. Relationship between single fan and multi-fans. Alluvial fan or fan delta is actually a complex of fans. The mudstones are deposited on the outer fan.

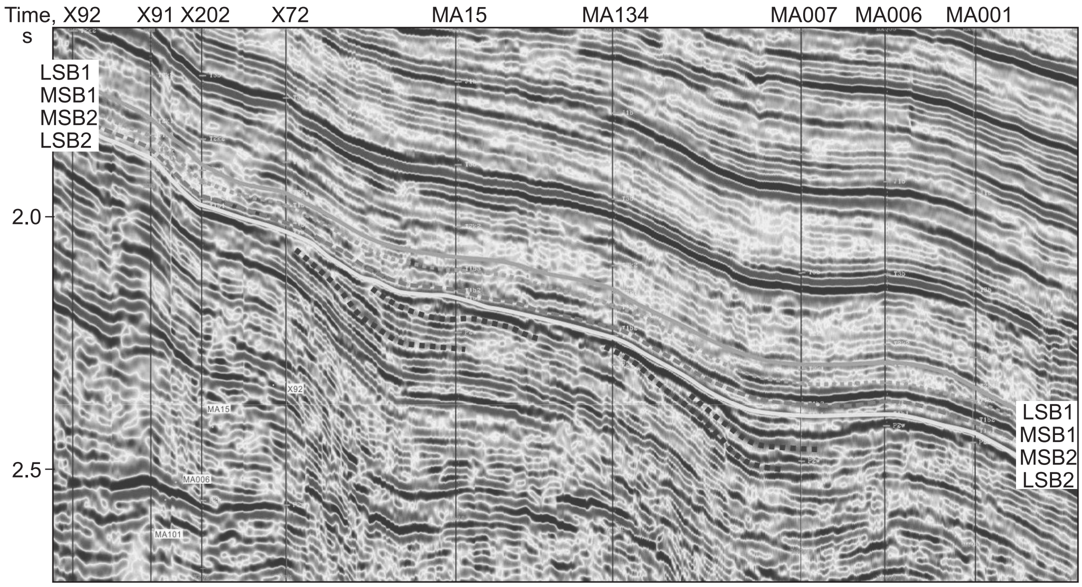

Fig. 10. Main sequence stratigraphic surfaces in the seismic section.

ited. When the energy is not enough to transport sediments into the lake, mudstones are deposited in the subaerial, causing the mudstones to oxidize, exhibiting such colors as brown, red, and yellow. The flume tank experiment and the analysis of the modern deposition system has revealed that the alluvial fan or fan delta is actually a complex of fans (Fig. 9). Each flood can form a new fan; the swing and superposition of these fans form the fan delta or alluvial fan (Fig. 9). Laterally, the mudstones are deposited on the outer fan (Fig. 9). Vertically, the mudstones are interbeded between conglomerates.

4.5 Conglomerate Shoal Facies

4.5.1 Description

The conglomerate shoal is characterized by grayish-green, well-sorted and clast-supported conglomerates. The sedimentary structures of conglomerate shoal facies include massive bedding (Fig. 5, G) or cross bedding and fragments of gastropod and bivalve. The color of the matrix in the conglomerates is gray-green. In the RT log curves, the conglomerate presents broad-amplitude box-shape or bell-shape patterns (Fig. 3). The porosity of conglomerates in this facies is usually 8 to 14%.

4.5.2 Interpretation

The well-sorted and clast-supported coarse-grained sediments indicate a relatively steady and continuous hydrodynamics. The common appearance of cross bedding and massive bedding in conglomerates is interpreted as having deposited in relative strong hydrodynamics. The fossils and the greyish-green conglomerates suggest that the depositional environment is subaqueous.

4.5.3 Formation

According to the flume tank experiment, the conglomerate shoal forms during the flood period which is dominated by the sheet flow. When the sheet flow prograde into the lake, the conglomerate shoal is deposited by the resistance from the water of the lake, and are reworked by offshore current and lake waves later. Laterally, this facies are distributed along the shoreline like a sheet (Fig. 7, A, C).

4.6 Sandy Shoal Facies

4.6.1 Description

The sandy shoal is characterized by well-sorted sandstones. The sedimentary structures of the sandy shoal include parallel bedding, grade bedding (Fig. 5, H) and cross bedding (Fig. 5, I). The single layer of this facies is usually less than five meters, and frequently interbeded with mudstone layers. The sandy shoal deposits have middle-amplitude tooth-like, funnel-shaped and bell-shaped curves in the RT log. The grain-size accumulation probability curve has three sub-populations, one rolling sub-population, one saltation sub-population and suspended sub-population (Fig. 6). The porosity of this facies is usually 8 to 14%.

4.6.2 Interpretation

The common appearance of cross bedding and parallel bedding in sandstones is considered as depositing in relatively strong hydrodynamics (Fraser & Hester, 1977; Clemmensen, 1978; Jiang, 2003; Tucker, 2003). The three sub-populations, one rolling sub-population, one siltation sub-population and one suspended sub-population, in the grain-size accumulation probability curve indicated that the sandy shoal was controlled by multiple currents, including offshore current and wave current.

4.6.3 Formation

According to the flume tank experiment, due to the decrease in velocity of the sheet flow and the effect of waves and longshore current, the sandstones are deposited between the conglomerate shoal and the prodelta (Fig. 7, C). During the flood period, the sheet flow provides the sandy shoal with the sediments; during the low flood period, the sandy shoal is reworded by wave and longshore currents.

4.7 Prodelta Facies

4.7.1 Description

The prodelta facies is characterized by greyish-green to dark mudstones (Fig. 5, J). Two types of mudstone are present. First one is thin (2m thick) and generally intercalated with siltstones. The other mudstone is thick (>2m). Observed sedimentary structure is horizontal laminations. Lateral distributions of this facies are stable. The prodelta deposits have short-amplitude tooth-like curves in the RT log (Fig. 3).

4.7.2 Interpretation

The dominance of mudstones in this facies indicates a low-energy environment. However, the thin-bed mudstones and thick-bed mudstones are deposited in different environments. The thin-bed mudstones with siltstones are considered as mudstones deposited near the wave base, whereas the thick-bed mudstones are considered as normal shallow lake mudstones deposited in a relative deeper water environment.

5. SEISMIC STRATIGRAPHY

The seismic stratigraphy in the study area started from an unconformities (LSB2), and consist of three seismic units. Generally, unconformities and their correlative conformities are used as sequence-bounding surfaces (Mitchum and Vail 1977) because they represent time-barrier surface. In seismic profiles, the unconformi-

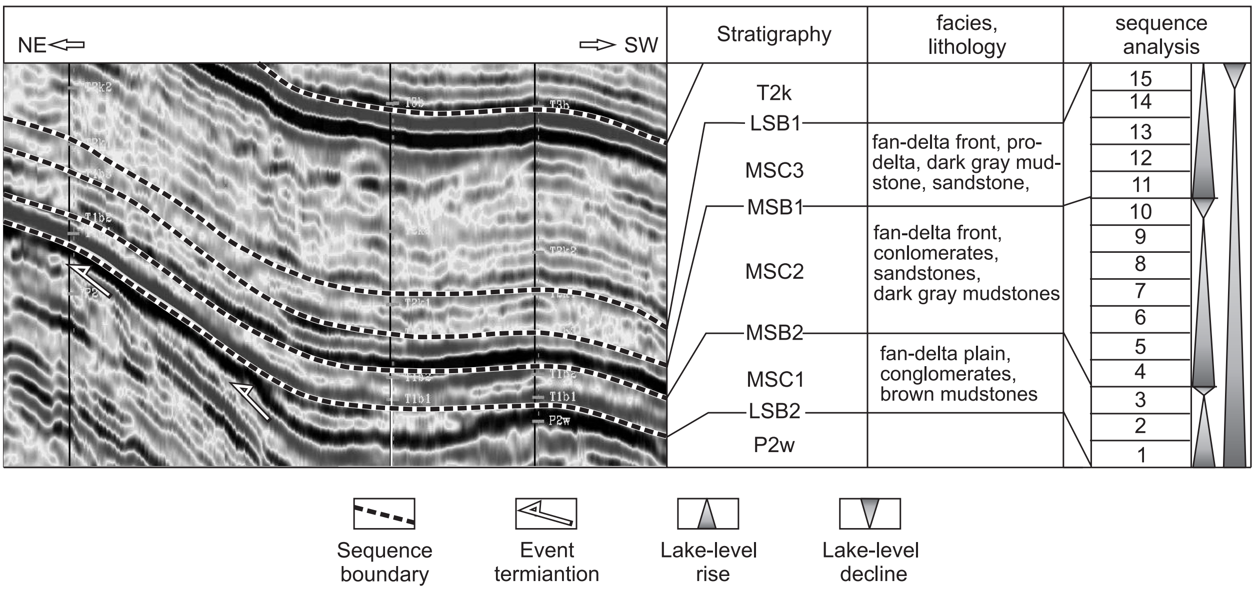

Fig. 11. Identification of main sequence stratigraphic surfaces and stratigraphic division frame work.

ties generally appear the erosional truncation (Fig. 10). Several strong amplitude well-continuity events represent three seismic units, indicating that there are strong reflectors on the top of each units (Fig. 10). The lower seismic unit that have been drilled corresponds to early Triassic conglomerates. The base of this unit is referred to as the unconformities (LSB2) (Fig. 10). The top of this unit are several meters of well-continuity mudstones named as horizon "MSB2". The middle seismic unit corresponds to conglomerates and sandstones. The top of this unit are several meters of well-continuity mudstones named as horizon "MSB1" (Fig. 10). The upper seismic unit that drilled corresponds to the upper Lower Triassic sandstones and mudstones. The top of this unit are several meters of well-continuity mudstones named as horizon "LSB1" (Fig. 10).

6. SEQUENCE STRATIGRAPHY

6.1 Sequence boundary

Identification of sequence boundaries and classification of depositional trends are the core part of multilevel stratigraphic correlation and division. Integrated seismic and well analysis shows that four major sequence boundaries are there collaboratively limiting the study area:

LSB1 (long-cycle sequence boundary 1), the top surface of the long-term base level cycle (LSC1) in the study area, has strong and continuous reflection on seismic section (Fig. 11). It is a regional parallel unconformity, and it is characterized by a thick and continuous mudstone layer of top T_1b. Its features on well logging curves are high gamma ray, acoustic, and spontaneous potential value and low resistivity value. This surface is also the top of an inverted triangle comprised of GR and RT curves which reveals the end of an overall fining-upward trend (Fig. 12).

LSB2 (long-cycle sequence boundary 2), the bottom surface of LSC1 in the study area, is an angle unconformable surface, and has strong and continuous reflection, and is the truncation on seismic section (Fig. 11). Its features on well logging curves are also high GR and low RT value (Fig. 12).

MSB1 (middle-cycle sequence boundary 1) and MSB2 (middle-cycle sequence boundary 2) are identified between LSB1 and LSB2. MSB1 and MSB2 are sedimentary discontinuities, and have strong and continuous reflection (Fig. 11), and are characterized by a thick and continuous mudstone layer in part area. Its features on well logging curves are also high GR and low RT value (Fig. 12). MSB1 and MSB2 separate LSB1 into three middle-term base level cycle, MSC1, MSC2 and MSC3.

6.2 Facies associations under sequence stratigraphic frame

LSC1 as a whole is a retrogradation cycle. From bottom to top, the color mudstone and muddy matrix in conglomerates gradually change from brown to dark grey; the grain size decreases gradually; the thickness of coarse-grained sediments decreases gradually; the thickness of mudstone increases gradually (Fig. 12). In the aspect of facies, from bottom to top, the fan-delta plain transforms into the fan-delta front gradually (Fig. 4, 12). The sedimentary stratigraphy shows a proximal-middle-distal trend, demonstrating an overall retrogradation stacking pattern (Fig. 4, 12). According to the oilfield development practice and stratigraphic reality, the study area could be divided into 15short-term base level cycles under the sequence stratigraphic frame limited by these sequence boundaries stated above (Fig. 11).

MSC1 is a secondary retrogradation cycle, comprising of short-term base level cycles 1 to 3, is the lower part of the study area and limited by the LSB2 at the bottom and the MSB2 at the top. MSC1 is mainly the fan-delta plain, dominated by conglomerate overbank facies with lenticular braided channel facies (Fig. 4, C, 12). The lithology is mainly conglomerate. The color mudstone and muddy matrix in conglomerates mainly is brown. The conglomerate/strata percentage of MSC1 is more than 80%; from bottom to top, the thickness of mudstone is increasing (Fig. 12).

MSC2 is a secondary retrogradation cycle, comprising of short-term base level cycles 4 to 10, is the middle part of the study area and limited by the MSB2 at the bottom and the MSB1 at the top. MSC2 mainly is the fan-delta front, dominated by conglomerate shoal facies and sandy shoal facies (Fig. 4, B, 12). The lithology is mainly conglomerate and sandstone. The color mudstone and muddy matrix in conglomerates mainly is dark grey. The conglomerate/strata percentage of MSC2 is more than 50%; from bottom to top, the thickness of mudstone is increasing (Fig. 12). The sedimentary stratigraphy shows a proximal-middle-distal trend, demonstrating an overall retrogradation stacking pattern.

MSC3 is a secondary retrogradation cycle, comprising of short-term base level cycles 11 to 15, is the upper part of the study area and limited by the MSB1 at the bottom and the LSB1 at the top. MSC3 mainly is the fan-delta front and prodelta, dominated by sandy shoal facies and prodelta mudstones (Fig. 4, A, 12). The lithology is mainly sandstone and mudstone. The conglomerate/strata percentage of MSC3 is less than 50%; from bottom to top, the thickness of mudstone is increasing (Fig. 12).

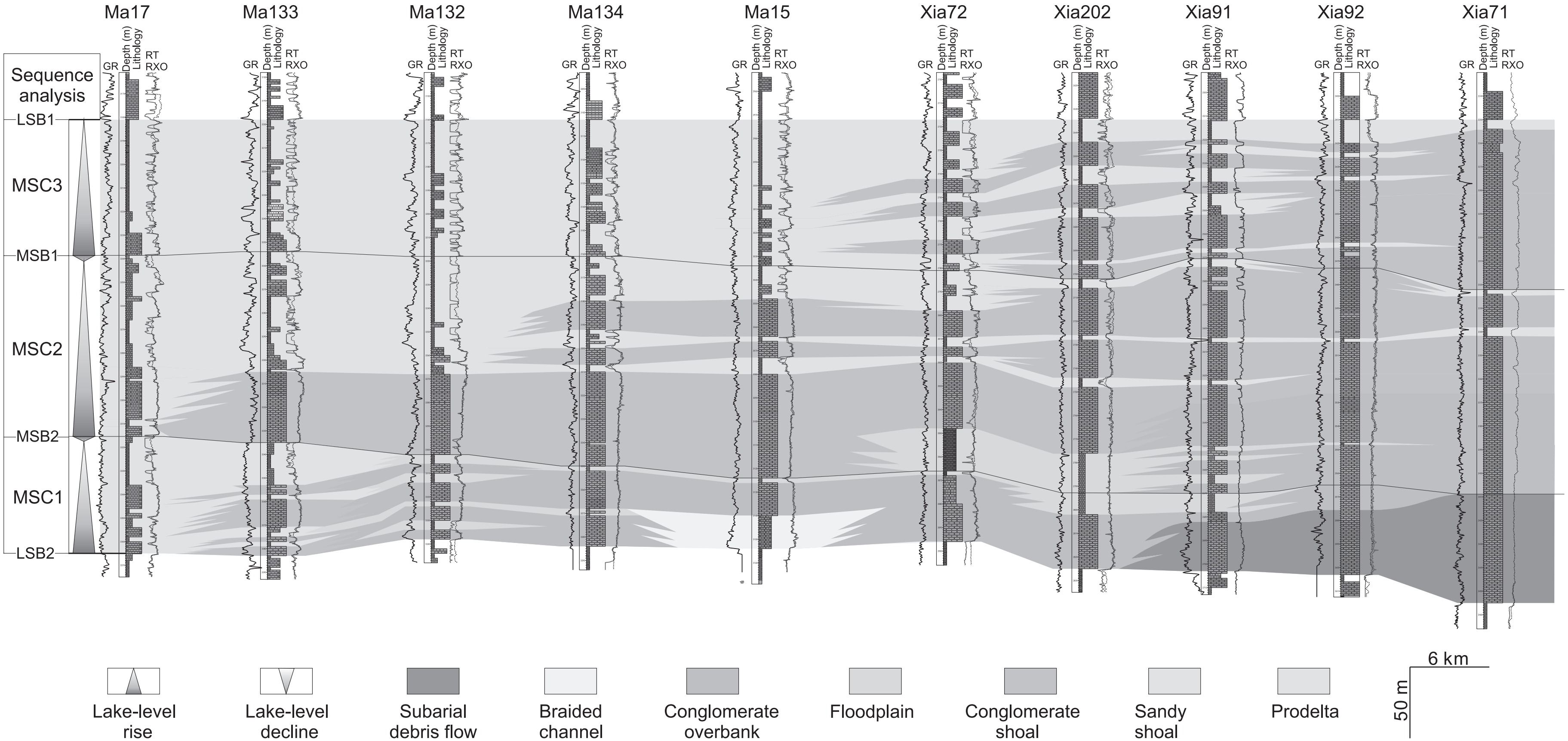

Fig. 12. Correlation section of LSC1in the Mabei area, Junggar basin, showing changes of the sedimentary facies.

7. DISCUSSION

7.1 Fan-delta sedimentary characteristics

According to previous researches about fan deltas, the fan delta depositional model made up by Galloway (1976) on the basis of Copper River fan delta was widely quoted, and Colella (1988) built up the fault-controlled marine Gilbert-type fan deltas, and so on. However, there are some different viewpoints or interpretations below against previous studies.

Many researchers showed that fan-delta plains are mainly composed of braided channels, and mudstones are interpreted as the deposition of the inter-channel in the fan-delta plain (Zou et al. 2015; Zhiwen et al. 2015; Xinghe et al. 2014; Jia et al; 2016). However, episodic overbank deposition is a dominant mechanism of delta plain aggradation (Shen et al. 2015). Fan-delta plains consist of alternations of sheet flow and channelized flow along the central line of deposition of the fan (Van Dijk et al. 2009; Wang et al. 2015). During the flood period, fan-delta plains are dominated by sheet flow, happened aggradation. During the low flood period, fan-delta plains are dominated by channelized flow, happened rework. Fan-delta plains are mainly composed of overbanks, and the inter-channel is characterized by the gravel or sand bodies form sheet flow.

Many researchers maintained that fan-delta front develop subaqueous channels (Olariu and Bhattacharya, 2006; Scholz et al., 1990; Shannon Jr and Dahl, 1971), and hold that the subaqueous channels are important reservoirs for hydrocarbon accumulation (Jia et al., 2016; Li et al., 2017; Yang et al., 2017). However, our study shows that there are no subaqueous channels in the fan-delta front, and most of clastic bodies in the fan-delta front are from the sheet flow occurred as a sheet rather than channelized characteristics.

7.2 Controls on sequence architecture

The sequence architecture and depositional evolution are mainly controlled by accommodation space, which might be the result of various factors such as tectonism, sea level change, and so on (Lin et al. 2001). Our study shows that the development of sequence architecture and depositional systems since the Lower Triassic in the study area are controlled by an interplay between lake level changes and sediment supply. During the Early Triassic, the Junggar basin was a closed lake (Wang 1994) and the tectonic activity was weak (Deng-Fa et al. 2004; Lei et al. 2005). The quickly rise of lake level and the creation of accommodation outpaced the rate of sediment supply result in a retrogradational fan-delta system.

7.3 Implication for hydrocarbon reservoir development

These different viewpoints can be a significant contribution to the reservoir interpretation within coarse-grained fan delta. The previous researchers showed that the subaqueous channels are important reservoir occurred as a belt in the fan-delta front, and it is not easy for the braided channels to form well reservoirs in the fan-delta plain, and the braided channels occupy most part of the fan-delta plain (Jia et al., 2016; Li et al., 2017; Yang et al., 2017). However, our study found that the important reservoirs in the fan-delta front are the conglomerate shoals and sandy shoals occurred as a sheet, and the braided channels are important reservoirs in the fan-delta plain occurred as a belt and occupying few part of the fan-delta plain. And the analysis of sequence stratigraphy indicates that the lake level change controls the distribution patterns of major reservoirs.

8. CONCLUSIONS

The Lower Triassic in the Mabei area is dominated by fan deltas, which is composed of fan-delta plain (including subaerial debris flow, braided channel, conglomerate overbank and floodplain), fan-delta front (including conglomerate shoal and sandy shoal) and prodelta. The braided channels form during the low flood period. The conglomerate overbanks form during the flood period, and occupy most part of fan-delta plain. The conglomerate shoals and sandy shoals form by the sheet flow which prograde into lakes, and are occurred as a sheet. The braided channels, conglomerate shoals and sandy shoals are easy to form high-porosity reservoirs.

The regional correlation of within the different depositional facies led to a sequence stratigraphic framework of 1 long-term base level cycles, 3 middle-term base level cycles and 15 short-term base level cycles. MSC1 is dominated by the fan-delta plain; MSC2 is dominated by the fan-delta front; MSC is dominated by fan-delta front and prodelta. The stratigraphy shows a proximal-middle-distal trend, demonstrating an overall retrogradation stacking pattern. The sequence architecture are controlled by an interplay between lake level changes and sediment supply. The quickly rise of lake level and the creation of accommodation outpaced the rate of sediment supply result in a retrogradational fan-delta system.

Acknowledgements

The subproject of Significant Science and Technology Special Projects of CNPC (NO.：2012E-34-01) partly funded this study. The authors thank the critical comments and suggestions from the Associate Editor and

Journal reviewer. The authors also thank our internal reviewers, Dr. Daiyan Zhang, for his constructive comments and suggestions.

REFERENCES

Burns, B.A., Heller, P.L., Marzo, M., Paola, C., 1997. Fluvial response in a sequence stratigraphic framework: example from the Montserrat fan delta, Spain. J. Sediment. Res. 67 (2), 311–321.

Carroll, A.R., Graham, S.A., Hendrix, M.S., Chu, J., McKnight, C.L. 1995. Late Paleozoic tectonic amalgamation of Northwestern China: Sedimentary record of the northern Tarim, northwestern Turpan, and southern Junggar basins. GSA Bull. 107 (5), 571–594.

Carroll, A.R., Yunhai, L., Graham, S.A., Xuchang, X., Hendrix, M.S., Jinchi, C., McKnight, C.L., 1990. Junggar basin, northwest China: trapped Late Paleozoic ocean. Tectonophysics 181(1–4), 1–14.

Catuneanu, O., 2006. Principles of Sequence Stratigraphy. Elsevier LTD, Oxford.

Celmmensen, L.B., 1978. Lacustrine facies and stromatolites from the Middle Triassic of East Greenland. J. Sediment. Petrol. 48 (4), 1111–1128.

Colella, A., 1988. Fault-controlled marine Gilbert-type fan deltas. Geology 72 (11), 1031–1034.

Deng-Fa, H.E., Yin, C., She-Kuan, D.U., Shi, X., Hui-Shu, M.A., 2004. Characteristics of structural segmentation of foreland thrust belts—A case study of the fault belts in the northwestern margin of Junggar Basin. Earth Sci. Front. 11 (3), 91–101.

Dortz, K.L., Meyer, B., Sйbrier, M., Braucher, R., Nazari, H., Benedetti, L., Fattahi, M., Bourlиs, D., Foroutan, M., Siame, L., 2011. Dating inset terraces and offset fans along the Dehshir Fault (Iran) combining cosmogenic and OSL methods. Geophys. J. Int. 185 (3), 1147–1174.

Evans, G., 1993. Stratigraphic Sequences and Their Chronostratigraphic Correlation: Discussion. J. Sediment. Res. 63(2), 304–305.

Feng, Y., Jiang, S., Wang, C., 2015. Sequence stratigraphy, sedimentary systems and petroleum plays in a low-accommodation basin: Middle to upper members of the Lower Jurassic Sangonghe Formation, Central Junggar Basin, Northwestern China. J. Asian Earth Sci. 105, 85–103.

Fraaser, G.S., Hester, N.C., 1977. Sediments and sedimentary structures of a beach-ridge complex, southwestern shore of Lake Michigan. J. Sediment. Petrol. 47 (4), 1187–1200.

Galloway, W.E., 1976. Sediments and stratigraphic framework of the Copper River fan-delta, Alaska. J. Sediment. Res. 46 (3), 726–737.

Galloway, W.E., 1989. Genetic stratigraphic sequences in basin analysis, I. Architecture and genesis of flooding-surface bounded depositional units. AAPG Bull. 73 (2), 125–142.

Gloppen, T.G., Steel, R.J., 1981. The deposits, internal structure and geometry in six alluvial fan–fan delta bodies (Devonian–Norway)—a study in the significance of bedding sequence in conglomerates, in: Ethridge, F.G., Flores, R.M. (Eds.), Recent and ancient non-marine depositional environments: Models for explorations. Special Publication 31. Society of Economic Paleontologists and Mineralogists, pp. 49–69.

Gуmez-Paccard, M., Lуpez-Blanco, M., Costa, E., Garcés, M., Beamud, E., Larrasoaña, J.C., 2012. Tectonic and climatic controls on the sequential arrangement of an alluvial fan/fan-delta complex (Montserrat, Eocene, Ebro Basin, NE Spain). Basin Res. 24 (4), 437–455.

He, D.F., Li, D., Fan, C., Yang, X.F., 2013. Geochronology, geochemistry and tectonostratigraphy of Carboniferous strata of the deepest Well Moshen-1 in the Junggar Basin, northwest China: Insights into the continental growth of Central Asia. Gondwana Res. 24 (2), 560–577.

Horton, B.K., Shmitt, J.G., 1996. Sedimentology of a lacustrine fan-delta system, Miocene Horse Camp Formation, Nevada, USA. Sedimentology 43 (1), 133–155.

Jia, H., Ji, H., Li, X., Zhou, H., Wang, L., Gao, Y., 2016. A retreating fan-delta system in the Northwestern Junggar Basin, northwestern China—Characteristics, evolution and controlling factors. J. Asian Earth Sci. 123, 162–177.

Jiang, Z., 2003. Sedimentology. Petroleum Industry Press, Beijing.

Larsen, V., Steel, R.J., 1978. The sedimentary history of a debris-flow dominated Devonian alluvial fan—a study of textural inversion. Sedimentology 25 (1), 37–59.

Li, Z., Zhang, L., Were, P., Wang, D., 2017. Sedimentary characteristics of 1st member of Yaojia Formation in Zhaoyuan-Taipingchuan region of Songliao Basin. J. Pet. Sci. Engin. 148, 52–63.

Lin, C., Eriksson, K., Li, S., Wan, Y., Ren, J., Zhang, Y., 2001. Sequence Architecture, Depositional Systems, and Controls on Development of Lacustrine Basin Fills in Part of the Erlian Basin, Northeast China. AAPG Bull. 85 (11), 268–269.

López-Blanco, M., Marzo, M., Piña, J., 2000. Transgressive–regressive sequence hierarchy of foreland, fan-delta clastic wedges (Montserrat and Sant Llorenç del Munt, Middle Eocene, Ebro Basin, NE Spain). Sedim. Geol. 138 (1), 41–69.

McConnico, T.S., Bassett, K.N., 2007. Gravelly Gilbert-type fan delta on the Conway Coast, New Zealand: Foreset depositional processes and clast imbrications. Sediment. Geol. 198 (3–4), 147–166.

Mitchum, R.M., 1985. Seismic stratigraphic expression of submarine fans. AAPG Mem. 39, 117–136.

Mitchum, R.M., Vail, P.R., 1977. Seismic stratigraphy and global changes of sea level, Part 7: Seismic stratigraphic interpretation procedure. AAPG Mem. 26, 135–143.

Nemec, W., Steel, R.J., 1984. Alluvial and coastal conglomerates: their significant features and some comments on gravelly mass flow deposits. CSPG Mem. 10, 1–31.

Olariu, C., Bhattacharya, J.P., 2006. Terminal distributary channels and delta front architecture of river-dominated delta systems. J. Sediment. Res. 76 (2), 212–233.

Pöppelreiter, M., Aigner T., 2003. Unconventional pattern of reservoir facies distribution in epeiric successions: Lessons from an outcrop analog (Lower Keuper, Germany). AAPG Bull. 87 (1), 39–70.

Park, M.E., Cho, H., Son, M., Sohn, Y.K., 2013. Depositional processes, paleoflow patterns, and evolution of a Miocene gravelly fan-delta system in SE Korea constrained by anisotropy of magnetic susceptibility analysis of interbedded mudrocks. Mar. Pet. Geol. 48, 206–223.

Posamentier, H.W., Summerhayes, C.P., Haq, B.U., Allen, G.P., 2009. An Overview of Sequence-Stratigraphic Concepts: Uses and Abuses, in: Posamentier, H.W., Summerhayes, C.P., Haq, B.U., Allen, G.P. (Eds.), Sequence Stratigraphy and Facies Associations. Blackwell Scientific, Oxford, pp. 1–18.

Scholz, C.A., Rosendahl, B.R., Scott, D.L., 1990. Development of coarse-grained facies in lacustrine rift basins: Examples from East Africa. Geology 18 (2), 140–144.

Shannon Jr., J.P., Dahl, A.R., 1971. Deltaic stratigraphic traps in west Tuscola field, Taylor County, Texas. AAPG Bull. 55 (8), 1194–1205.

Shen, Z., Törnqvist, T.E., Mauz, B., Chamberlain, E.L., Nijhuis, A.G., Sandoval, L., 2015. Episodic overbank deposition as a dominant mechanism of floodplain and delta-plain aggradation. Geology 43 (10), 875–878.

Song, Y.D., Dai, J.S., Kong-You, W.U., 2009. Study on the structural features and hydrocarbon accumulation modes of Wuxia fault belt in the northwest margin of Junggar Basin. J. Xian Shiyou University.

Tucker, M.E., 2003. Sedimentary Rocks in the Field. John Wiley & Sons Ltd, West Sussex.

Van Dijk, M., Postma, G., Kleinhans, M.G., 2009. Autocyclic behaviour of fan deltas: an analogue experimental study. Sedimentology 56 (5), 1569–1589.

Visher, G.S., 1969. Grain size distributions and depositional processes. J. Sediment. Petrol. 39 (3), 1074–1106.

Wang, J., Jiang, Z., Zhang, Y., Gao, L., Wei, X., Zhang, W., Liang, Y., Zhang, H., 2015. Flume tank study of surface morphology and stratigraphy of a fan delta. Terra Nova 27 (1), 42–53.

Wang, L., 1994. Approaches to the curves for the lakelevel fluctuations in the Junggar basin during Meso-Cenozoic time. Sediment. Facies Palaeogeogr. 14 (6), 1–14.

Whipple, K.X., Dunne, T., 1992. The influence of debris-flow rheology on fan morphology, Owens Valley, California. GSA Bull. 104 (7), 887–900.

Xian, B., Xu, H., Jin, Z., Wang, C., Lu, Y., Huang, L., 2008. Sequence stratigraphy and subtle reservoir exploration of Triassic system in northwestern margin of Junggar basin. Geol. J. China Universities 14 (2), 139–146.

Xinghe, Y.U., Jianhua, Q.U., Tan, C., Zhang, L., Xiaolu, L.I., Gao, Z., 2014. Conglomerate lithofacies and origin models of fan deltas of Baikouquan Formation in Mahu Sag, Junggar Basin. Xinjiang Pet. Geol. 35 (6), 619–627.

Yang, R., Jin, Z., van Loon, A.T., Han, Z., Fan, A., 2017. Climatic and tectonic controls of lacustrine hyperpycnite origination in the Late Triassic Ordos Basin, central China: implications for unconventional petroleum development. AAPG Bull. 101 (1), 95–117.

Yuanjiang, Y.U., Desheng, L.I., Suyun, H.U., Lei, Z., He, D., 2007. Fans sedimentation and exploration direction of fan hydrocarbon reservoirs in foreland thrust belt of the Northwestern Junggar Basin. Acta Geosci. Sin. 28 (1), 62–71.

Zecchin, M., Catuneanu, O., 2015. High-resolution sequence stratigraphy of clastic shelves III: Applications to reservoir geology. Mar. Pet. Geol. 62, 161–175.

Zhao, B., 1992. Formation and evolution of Junggar Basin. Xinjiang Pet. Geol. 13, 191–196.

Zhang, J., Li, J., Liu, S., Li, C., 2015a. Sedimentology and sequence stratigraphy of the second member of Shuangyang Formation, Y45 Block, Moliqing oilfield, Yitong Basin, China. Arabian J. Geosci. 8 (9), 6697–6707.

Zhang, S., Zou, N., Shi, J., Chang, Q., Lu, X., Chen, B., 2015b. Depositional model of the Triassic Baikouquan Formation in Mabei area of Junggar Basin. Oil Gas Geol. 36 (4), 640–650.

Zhenyu, L., Bing, L., Yuanjiang, W., Liping, Z., Xin, S., 2005. Tectonic evolution and development and distribution of fans on northwestern edge of Junggar Basin. Oil Gas Geol. 1, 11.

Zhiwen, Z., Hui, L., Yang, X., Chaofeng, Y., Xiangchao, M. 2015. Sedimentary characteristics of the Baikouquan Formation, Lower Triassic in the Mahu Depression, Junggar Basin. Geol. Sci. Technol. Inform. 2 (34), 20–26.

Zou, C., Hou, L., Kuang, L., Kuang, J., 2007. Genetic mechanism of diagenesis-reservoir facies of the fan-controlled Permo-Triassic in the western marginal area, Junggar basin. Chinese J. Geol. (Scientia Geol. Sin.) 42 (3), 587–601.

Zou, N.N., Shi, J.A., Zhang, D.Q., Ma, C.Y., Zhang, S.C., Xinchuan, L.U., 2015. Fan delta depositional model of Triassic Baikouquan Formation in Mabei Area, NW Junggar Basin. Acta Sediment. Sin. 33 (3), 607–615.

Рекомендована к печати 2 августа 2017 г.
Н.В. Сенниковым

Поступила в редакцию
29 апреля 2017 г.